W-Band Subharmonic Mixer with Silica-Based Post-Wall Waveguide Interface

Thuroczy, Tomas; Zhurbenko, Vitaliy; Johansen, Tom Keinicke; Uemichi, Yusuke; Nukaga, Osamu; Okude, Satoshi; Guan, Ning

Published in:
Progress in Electromagnetics Research Letters

Publication date:
2020

Document Version
Publisher's PDF, also known as Version of record

Progress In Electromagnetics Research Letters, Vol. 90, 105–111, 2020

W-Band Subharmonic Mixer with Silica-Based Post-Wall Waveguide Interface

Tomas Thuroczy[1, *], Vitaliy Zhurbenko[1], Tom K. Johansen[1], Yusuke Uemichi[2], Osamu Nukaga[2], Satoshi Okude[2], and Ning Guan[2]

Abstract—This paper presents the design of a compact size, passive, W to K band subharmonic mixer with post-wall waveguide (substrate integrated waveguide) RF input interface. The mixer is based on a silica-glass structure where the post-wall waveguide and microstrip line are on separate substrates. This configuration maximizes the performance as the substrate thicknesses can be separately optimized for the lowest loss and mono-mode operation. Integration of different types of guiding structures also allows realization of e.g., millimetre-wave waveguide filters and microstrip circuits in a single structure, while preserving low-cost, low-weight and compact size. Furthermore, post-wall waveguides can be easily interfaced with conventional rectangular waveguides, as demonstrated in the paper, which simplifies millimeter-wave circuit packaging and eventual system integration. Design methodology of the mixer and transition circuits as well as measurements are presented. Minimum conversion loss of 19.6 dB was achieved at 86 GHz with 13.7 dBm/32.4 GHz LO signal. The presented design would be suitable for the future W-band cellular, radar, or satellite communication systems.

1. INTRODUCTION

W-band (75–110 GHz) and E-band (60–90 GHz) will play an important role in the future cellular (such as 5G), radar, and spaceborne communication systems. Meeting performance requirements of millimeter-wave systems often requires integration of different guiding structures. Air-filled rectangular waveguide is common for antenna interfaces, whereas post-wall waveguides (PWW) are very suitable for realizing low-loss millimeter-wave filters (e.g., [8], [9], [10]), antennas ([7]) or other circuits. For instance, the PWW-based filters can outperform the microstrip equivalents in terms of Q-factor, which in turn yields better selectivity [6]. Furthermore, millimeter-wave filters designed using this silica-based PWW have superior thermal stability, compared to the standard rectangular waveguide filters [10]. In the antenna domain, microstrip patch antenna arrays suffer from low efficiency at millimeter-wave frequencies due to conductor losses and radiation losses of the feeding network [18]. A suitable and more efficient alternative is a planar slotted waveguide antenna array in a post-wall waveguide structure [7]. Planar circuitry is mostly realized using microstrip lines. Creating low-loss transitions between these structures while preserving compact size of the device is desirable for integration purposes.

Several W-band passive subharmonic mixers based on Schottky diodes have been proposed and built (e.g., [1], [4] or [5]) based on a microstrip or coplanar waveguide input interface. This work presents a W-band subharmonic mixer with silica-based post-wall waveguide RF input interface. The circuit is fabricated on a single integrated structure that supports both the silica-based PWW and microstrip line. The mixer is based on an anti-parallel diode pair (APDP) topology operating in a subharmonic mode, thus relaxing the LO frequency requirement. APDP topology has the advantages of rejecting the fundamental mixing product, suppressing AM noise in the LO signal and higher output spectral purity

Received 22 January 2020, Accepted 6 April 2020, Scheduled 11 April 2020
* Corresponding author: Tomas Thuroczy (tthuroczy@xmotx.net).
[1] Technical University of Denmark, Denmark. [2] Fujikura Ltd., Japan.

due to inherent rejection of even order mixing products [14]. Opposed to an active MMIC solutions, passive mixer has zero power consumption, however at the expense of higher conversion loss.

The paper is organized as follows: Section 2 describes the used guiding structures and transition circuits between them. Section 3 demonstrates the subharmonic mixer design, and Section 4 presents the measured results. Conclusions are presented in the Section 5.

2. GUIDING STRUCTURES AND TRANSITIONS

2.1. Guiding Structures

The proposed mixer is realized on a silica glass block that incorporates both the PWW and microstrip line. The former serves as an RF input for the mixer, and the latter contains planar circuitry and IF/LO signal ports.

The vertical stack of the structure is shown in the Fig. 1. The PWW is created by placing metallic walls on the top and the bottom of the silica glass substrate and creating rows of metallic posts along it. The diameter and spacing between the posts are 100 µm and 200 µm, respectively. The parameters of the silica glass substrate which were used in the design are: thickness 500 µm, $\varepsilon_r = 3.814$@60 GHz and $\tan\delta = 0.000542$@60 GHz. Microstrip line is realized by placing a thin film resin, serving as a substrate, on top of the PWW's metallic wall, as depicted in Fig. 1. Another layer of copper forming the signal trace is placed on the resin's top.

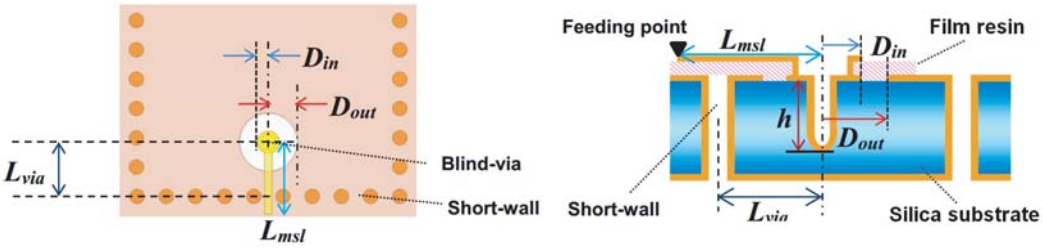

Figure 1. Top view and side view of the silica/resin stack and the blind-via apparatus (courtesy of Fujikura).

Modal analysis of the PWW reveals that only TE_{m0} modes are supported, as other modes require longitudinal current flow on the side walls, which is not possible due to their discontinuity [11]. Treating the PWW as a rectangular waveguide with width a, height b and dielectric filling ε_r allows calculating approximate cutoff frequencies of the TE_{m0} modes as follows:

$$f_{c_{mn}} = \frac{1}{2\pi\sqrt{\mu\varepsilon_r}}\sqrt{\left(\frac{m\pi}{a}\right)^2 + \left(\frac{n\pi}{b}\right)^2} \tag{1}$$

More accurate estimation of the $f_{c_{mn}}$ requires calculating the effective PWW width which accounts for the discontinuous side walls. The effective width usually lies between a and $a - d$ where d is a diameter of the post [11].

The designed PWW has a width of 1.5 mm which approximately results in f_{TE10} of 53 GHz and f_{TE20} of 106 GHz. This configuration ensures monomode operation in the band of interest (81–86 GHz).

2.2. Transition Circuits

2.2.1. WR-10 to PWW

Air-filled rectangular waveguide is a common interface of various measuring equipment and antennas. Transition from the WR-10 to the PWW is based on inserting a quarter-wave section between the waveguides. Equivalent characteristic impedance of a waveguide can be calculated by use of the *modified power-voltage definition*, which takes following form [15]

$$Z_0 = 377\,\frac{b}{a}\sqrt{\frac{\mu_r}{\varepsilon_r}}\,\frac{\lambda_g}{\lambda} \quad \text{where} \quad \frac{\lambda_g}{\lambda} = \frac{1}{\sqrt{1-(f_c/f)^2}} \tag{2}$$

This definition allows calculating waveguide characteristic impedance depending on its geometrical size and type of the dielectric filling. If we denote Z_1 and Z_3 as characteristic impedances of the WR-10 and PWW, corresponding quarter-wave waveguide section should have a characteristic impedance of $Z_2 = \sqrt{Z_1 Z_3}$ [16]. Once Z_2 is known, physical size of the quarter-wave section can be derived from Eq. (2). However, additional EM optimization is required to achieve desired performance as parasitic inductances and capacitances arising from geometrical changes in the width and height between different waveguides are not taken into account.

The designed transition including the physical dimensions is shown in Figs. 2(a) and 2(b). Impedance of the matching section is controlled by changing the height and fixing the width.

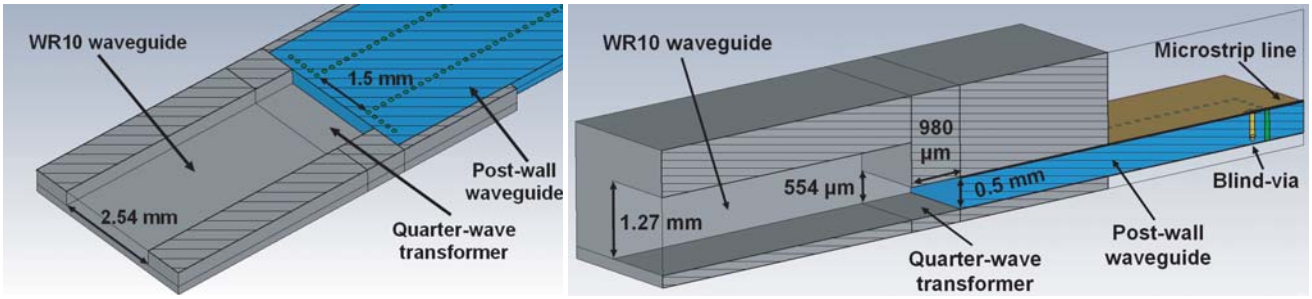

(a) (b)

Figure 2. Horizontal and vertical cut of WR-10 to post-wall waveguide transition.

2.2.2. PWW to Microstrip

As outlined in the introduction, integration of microstrip line and post-wall waveguide has the advantage of realizing waveguide circuits together with microstrip circuits in a compact structure. In order to maximize the performance of each, it is necessary to minimize the insertion loss and ensure mono-mode operation. At the same time, low-loss transition between the two is desired. For the microstrip line, it is desirable to keep the thickness of the substrate low, in order to prevent excitation of higher-order modes and minimize the amount of radiation [12, 17]. On the contrary, the loss of the rectangular waveguide and PWW increases with decreasing thickness [13]. Therefore, the thickness of the PWW should be optimized for low insertion loss as well as rejection of the higher order modes. The proposed two layer structure (Fig. 1) is suitable for this purpose as the thickness requirements for both the microstrip line and PWW can be simultaneously fulfilled on separate substrates.

Transition from PWW to microstrip line is realized by inserting a blind-via, connected to a microstrip line, into the PWW's substrate as depicted in Fig. 1. Blind-via works similarly as an E-plane probe in an air-filled rectangular waveguide and is placed approximately $\lambda_g/4$ away from the PWW's wall.

CST simulated insertion loss and matching of the end-to-end transition (WR-10 to PWW to microstrip) is shown in Fig. 3(a). Physical lengths of the WR-10 waveguide, post-wall waveguide and microstrip line are 37 mm, 6 mm and 1 mm, respectively. The transition exhibits 0.8 dB of loss and better than -15 dB matching in approximately 10 GHz of bandwidth. The resin substrate is the main contributor to the total loss. Physical dimensions of the transition, with respect to the notation in the Fig. 1, are as follows: $L_{msl} = 1000\,\mu$m, $L_{via} = 300\,\mu$m, $D_{in} = 100\,\mu$m, $D_{out} = 150\,\mu$m, $h = 450\,\mu$m. Transition circuits 2.2.1 and 2.2.2 were modelled and optimized in the CST Studio, using the time-domain solver.

3. SUBHARMONIC MIXER DESIGN

The basic subharmonic mixer topology is shown in Fig. 3(b) and is similar to the ones employed in [1] or [2]. Center frequencies for the RF, LO and IF signals are 83.5 GHz, 32.4 GHz and 18.7 GHz, respectively. The mixer is based on anti-parallel diode pair (APDP) connection which is very suitable

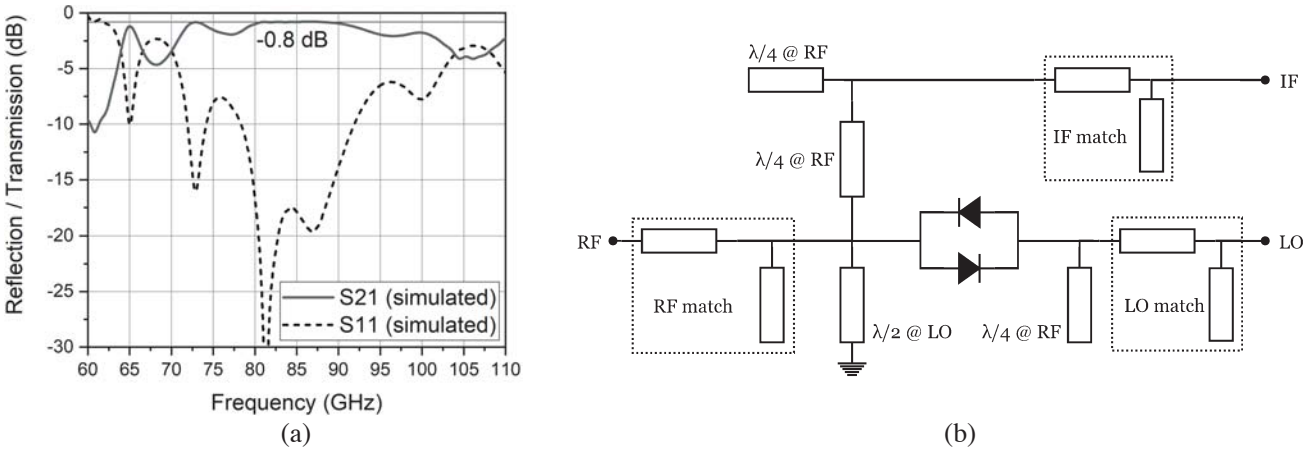

Figure 3. (a) Simulated end-to-end transition from WR-10 waveguide to PWW to microstrip line. (b) Block diagram of the designed subharmonic mixer.

for subharmonic operation, as it inherently suppresses the fundamental mixing product as well as even order mixing products and even harmonics of the LO [3]. APDP is formed by using two discrete Macom MA4E1310 Schottky diodes. Dimension of each diode is approximately 330 µm × 660 µm. The total capacitance and series resistance of the diode are 0.04 pF and 6 Ohm, respectively. The remaining diode parameters used in the simulations were taken from data provided by Macom. The mixer was simulated and optimized in Keysight ADS using the Harmonic Balance simulator together with Momentum EM solver. The CST simulation result of the transition circuits was exported as a touchstone file and placed in the RF port of the mixer in the Keysight ADS simulator.

The mixer circuitry contains matching networks, return paths, soldering pads, and probing pads. The two $\lambda_{RF}/4$ transmission lines in the IF branch create an open circuit condition for the RF signal, thus preventing its leakage into the IF port. The grounded $\lambda_{LO}/2$ stub serves as a DC return path and a return for the LO signal, which improves the LO-to-IF isolation. The open-circuited $\lambda_{RF}/4$ stub behind the diodes is a return path for the RF signal and prevents the leakage into the LO port. WR-10 RF input interface, with cutoff frequency above the IF and LO signals, inherently provides LO-to-RF and IF-to-RF isolations. Furthermore, it provides an open circuit termination for the image frequency, located at 46.1 GHz.

4. MEASUREMENTS

The manufactured mixer circuit is shown in Fig. 4. The total size of the silica glass structure (including the PWW) is $12 \times 4\,\text{mm}^2$. The size of the mixer circuit on it is approximately $2.2 \times 2.7\,\text{mm}^2$. The two Schottky diodes were manually soldered using the *Indalloy Solder Research Kit* from *Indium*

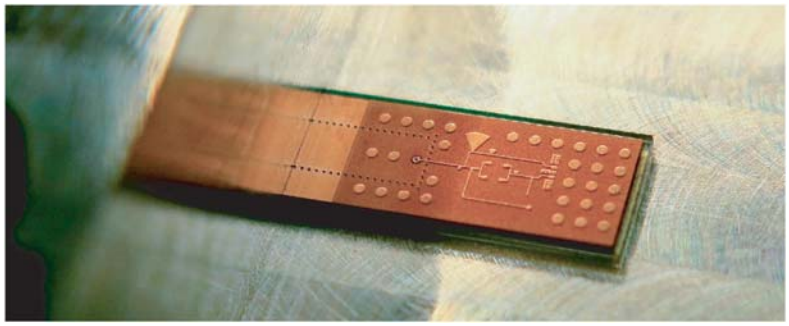

Figure 4. Fabricated structure inserted into the waveguide transformer (without the diodes mounted).

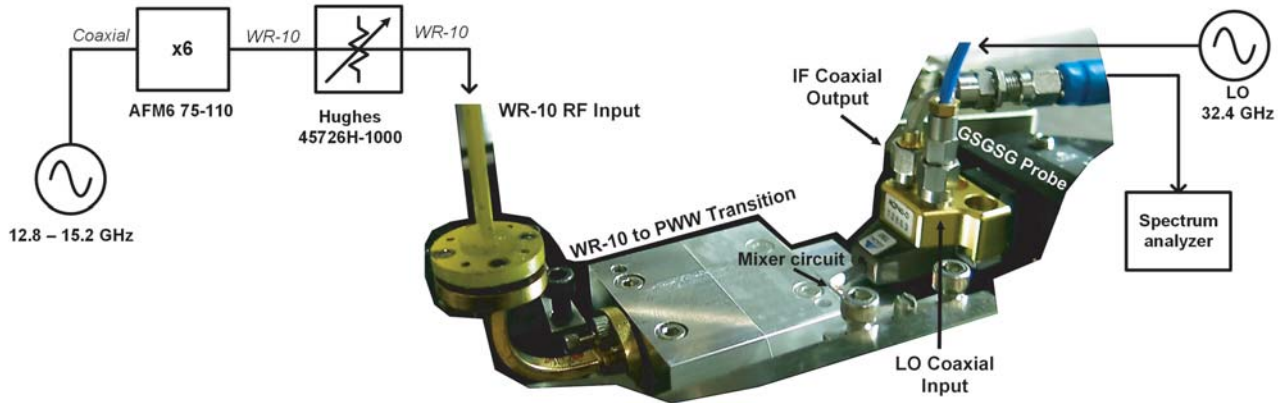

Figure 5. Block diagram and picture of the test setup.

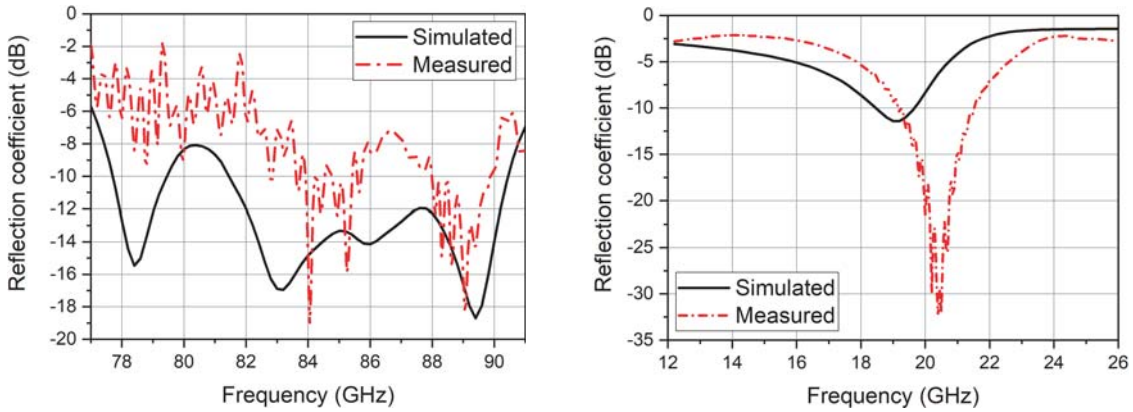

Figure 6. Measured and simulated RF and IF port matching. (a) RF port matching. (b) IF port matching.

Corporation. The used solder type #42 (46Bi/34Sn/20Pb) together with the flux #5RA from the kit have the advantage of low-temperature melting point, which reduces the thermal stress on the diodes. Access to the LO and IF ports is via the ground-signal-ground-signal-ground (GSGSG) probing interface with 150 µm pitch.

Conversion gain, impedance matching of the ports, and isolation measurements were performed. The test setup is shown in Fig. 5. Results of the RF and IF port matching are shown in Figs. 6(a) and 6(b). The higher measured RF return loss compared to the simulations could be attributed to an imperfect tight contact between the milled waveguide transformer and the PWW. In fact, additional CST simulations revealed that presence of air-gaps between the transformer (Fig. 2(a)) and the PWW causes some deterioration of the impedance matching. A frequency offset in the tuning of the IF matching network is likely due to an overestimated relative permittivity of the substrate.

For the conversion gain measurement, the W-band RF signal was generated by a Ku-band frequency synthesizer followed by an active x6 frequency multiplier *AFM6 75-110* which was connected to the WR-10 waveguide attenuator *Hughes 45726H-1000*. This chain generated a −30 dBm W-band signal which was fed into the input of the WR-10 to PWW transformer. Output power was verified with the Erickson PM5 power meter. The injection of the LO signal and extraction of the IF signal was via a *Dual Infinity* GSGSG probe from *Cascade Microtech*. Output power at the IF frequency was measured with a spectrum analyzer. The measured and simulated conversion gain versus RF frequency is shown in Fig. 7(a) and versus LO power in Fig. 7(b). Maximum conversion gain of −19.6 dB was achieved at 86 GHz with 13.7 dBm of LO power. The narrow conversion gain bandwidth is mainly due

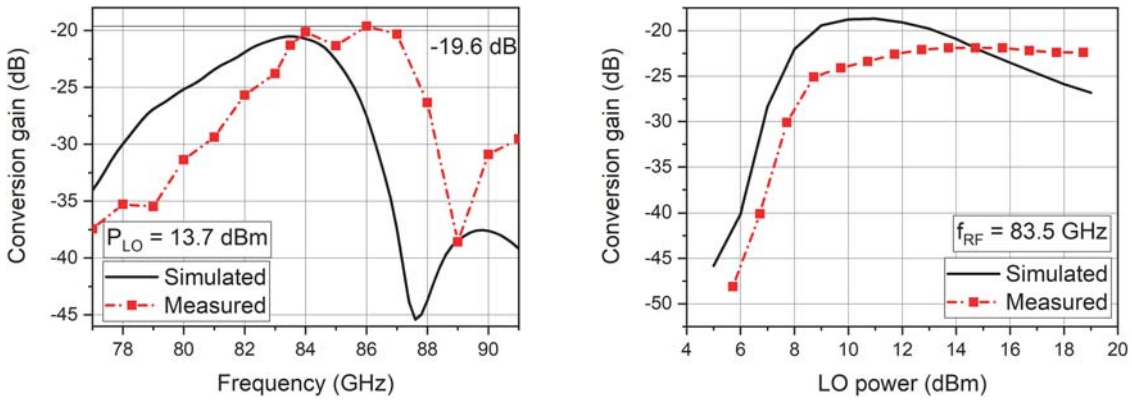

Figure 7. Measured and simulated conversion gain versus RF frequency and LO power.

to the narrow IF matching bandwidth as visible from the Fig. 6(b). Post-measurement analysis and simulations revealed that the microstrip line connected to the blind via transforms an open-circuit input impedance at the IF frequency to a low value. Subsequently, this affects the input impedance at the IF port and makes it difficult to match over a wide bandwidth, due to the Bode-Fano limit. Therefore, in the future design iterations, the microstrip line length from the blind via should be more carefully adjusted to preserve an open-circuit impedance for the IF frequency. A frequency offset of the conversion gain curve is due to the frequency offset of the IF matching network. The measured LO-to-IF isolation was −19 dB. The simulated RF-to-LO and RF-to-IF isolations are −18.8 and −21 dB, respectively. Simulated $P_{1\,\mathrm{dB}}$ compression point is +14 dBm. A comparison of different W-Band subharmonic mixers is in Table 1.

Table 1. Comparison of W-band subharmonic downconverting mixers.

Ref.	Technology	$G_{cnv,\max}$ [dB]	RF [GHz]	IF [GHz]	P_{LO} [dBm]
This work	WR-10 + PWW + Microstrip	−19.6	81–86	19–21.5	13.7
[5]	WR-10 + Microstrip	−22.3	85–95	9	10
[4]	WR-10 + Q-MMIC	−8	75–110	DC-18	10
[1]	CPW	−7	83–96	2–4	8.5

5. CONCLUSIONS

A W-band passive subharmonic mixer with post-wall waveguide interface was designed, manufactured, and measured. The peak conversion gain of −19.6 dB was achieved at the RF frequency of 86 GHz with 13.7 dBm/32.4 GHz LO signal. The mixer was built on a silica glass structure where microstrip line and post-wall waveguide have separate substrates. This arrangement allows minimizing the loss of both guiding structures and ensures mono-mode operation. Integrating the silica-based post-wall waveguide circuits with planar circuits based on thin film microstrip lines is suitable for designing future hybrid millimeter-wave systems.

ACKNOWLEDGMENT

The author would like to thank Fujikura Ltd. Japan for fabrication of the prototypes and DTU mechanical workshop for milling the waveguide transformer split-block.

REFERENCES

1. Raman, S., F. Rucky, and G. M. Rebeiz, "A high-performance W-band uniplanar subharmonic mixer," *IEEE Transactions on Microwave Theory and Techniques*, Vol. 45, No. 6, 955–962, Jun. 1997.
2. Xue, Q., K. M. Shum, and C. H. Chan, "Low conversion-loss fourth subharmonic mixers incorporating CMRC for millimeter-wave applications," *IEEE Transactions on Microwave Theory and Techniques*, Vol. 51, No. 5, 1449–1454, May 2003.
3. Cohn, M., J. E. Degenford, and B. A. Newman, "Harmonic mixing with an antiparallel diode pair," *IEEE Transactions on Microwave Theory and Techniques*, Vol. 23, No. 8, 667–673, Aug. 1975.
4. Xu, Z., Y. Cui, J. Xu, J. Guo, and C. Qian, "Low cost W-band sub-harmonic mixer using quasi-MMIC technology," *2015 IEEE International Wireless Symposium (IWS 2015)*, 1–4, Shenzhen, 2015.
5. Fujiwara, K. and T. Kobayashi, "Low-cost W-band frequency converter with broad-band waveguide-to-microstrip transducer," *2016 Global Symposium on Millimeter Waves (GSMM) & ESA Workshop on Millimetre-Wave Technology and Applications*, 1–4, Espoo, 2016.
6. Grine, F., T. Djerafi, M. T. Benhabiles, K. Wu, and M. L. Riabi, "High-Q substrate integrated waveguide resonator filter with dielectric loading," *IEEE Access*, Vol. 5, 12526–12532, 2017.
7. Chen, X., K. Wu, L. Han, and F. He, "Low-cost high gain planar antenna array for 60-GHz band applications," *IEEE Transactions on Antennas and Propagation*, Vol. 58, No. 6, 2126–2129, Jun. 2010.
8. Uemichi, Y., et al., "Compact and low-loss bandpass filter realized in silica-based post-wall waveguide for 60-GHz applications," *2015 IEEE MTT-S International Microwave Symposium*, 1–3, Phoenix, AZ, 2015.
9. Uemichi, Y., et al., "A 60-GHz six-pole quasi-elliptic bandpass filter with novel feeding mechanisms based on silica-based post-wall waveguide," *2017 IEEE MTT-S International Microwave Symposium (IMS)*, 1282–1284, Honololu, HI, 2017.
10. Uemichi, Y., O. Nukaga, X. Han, K. Kobayashi, S. Amakawa, and N. Guan, "Temperature dependence of bandpass filters built of silica-based post-wall waveguide for millimeter-wave applications," *2018 48th European Microwave Conference (EuMC)*, 703–706, Madrid, 2018.
11. Xu, F. and K. Wu, "Guided-wave and leakage characteristics of substrate integrated waveguide," *IEEE Transactions on Microwave Theory and Techniques*, Vol. 53, No. 1, 66–73, Jan. 2005.
12. Deslandes, D. and K. Wu, "Integrated transition of coplanar to rectangular waveguides," *2001 IEEE MTT-S International Microwave Symposium Digest*, (Cat. No.01CH37157).
13. Yeap, K. H., C. Y. Tham, G. Yassin, and K. C. Yeong, "Propagation in lossy rectangular waveguides," *Electromagnetic Waves Propagation in Complex Matter*, Ahmed Kishk, IntechOpen, Jul. 5, 2011.
14. Maas, S. A., *Microwave Mixers*, Artech House, 1986.
15. Rizzi, P. A., *Microwave Engineering: Passive Circuits*, Prentice Hall, 1988.
16. Pozar, D. M., *Microwave Engineering*, Wiley, 2017.
17. Bahl, I. J., M. Bozzi, and R. Garg, *Microstrip Lines and Slotlines*, 3rd Edition, Artech House, 2013.
18. Garg, R., P. Bhartia, I. J. Bahl, and A. Ittipiboon, *Microstrip Antenna Design Handbook*, Artech House, 2001.